Geotech Geol Eng (2017) 35:1–28
DOI 10.1007/s10706-016-0091-x

STATE-OF-THE-ART REVIEW

A Review of Seismic Damage of Mountain Tunnels and Probable Failure Mechanisms

Nishant Roy · Rajib Sarkar

Received: 31 December 2015 / Accepted: 12 September 2016 / Published online: 17 September 2016

Abstract Severe cases of damages of mountain tunnels following 1995 Hyogoken-Nanbu (Japan), 1999 Chi-Chi (Taiwan), 2004 Mid-Niigata Prefecture (Japan) and 2008 Wenchuan (China) earthquakes have challenged the traditional belief of tunnel structures being seldom damaged in seismic events. These experiences are a reminder that seismic behaviour of mountain tunnels must be further studied in detail. Such investigations assume greater significance as more number of tunnels are being planned to be constructed to meet the infrastructural needs of mountainous regions all around the world. In this paper, seismic damages of mountain tunnels have been reviewed. Prominent failure patterns have been identified based on the case histories of damages. Damages in the form of cracking of tunnel lining, portal cracking, landslide induced failures, uplift of bottom pavement, failures of sidewalls, shearing failure of tunnel liner and spalling of concrete have been majorly observed. Based on the damage patterns and earthquake data, main factors leading to instabilities have been discussed. Probable failure mechanisms of mountain tunnels under seismic loading conditions have been explained. Seismic analyses of a circular lined tunnel in blocky rock mass have been carried out through discrete element based approach. The significant role of different seismic parameters like frequency, peak ground acceleration has been identified. Moreover, effect of tunnel depth on the seismic response of tunnels has been investigated. It is believed that the present study will help in advancing the present state of understanding with regard to the behavior of tunnels under seismic conditions.

Keywords Mountain tunnel · Seismic damage · Failure mechanism · Case histories

N. Roy
Department of Civil Engineering, Malaviya National Institute of Technology Jaipur, Jaipur, India
e-mail: nishantciv@gmail.com

R. Sarkar (✉)
Department of Civil Engineering, Indian Institute of Technology (Indian School of Mines) Dhanbad, Dhanbad, India
e-mail: rajibdeq@gmail.com

1 Introduction

Driven by the increasing need of providing infrastructural facilities in mountainous regions, the construction of tunnels for highway and railway networks has witnessed a constant increase. Major tunneling projects are either being planned or being executed in more challenging and complex conditions than in the past. However, following recent seismic events, the traditional view with regard to earthquake resistant characteristics of tunnels as a whole have been challenged. Severe cases of damages of mountain tunnels have been reported in the 1995 Hyogoken-Nanbu (Japan), 1999 Chi-Chi (Taiwan), 2004 Mid-

Niigata Prefecture (Japan) and the 2008 Wenchuan (China) earthquakes (Asakura and Sato 1998; Otsuka et al. 1997; Wang et al. 2001; Shimizu et al. 2007b; Jiang et al. 2010; Li 2012; Chen et al. 2012; Shen et al. 2014 etc.). Such poor performances have led scholars and engineers to take up research in the area of seismic behaviour of tunnel and underground facilities (Kontoe et al. 2008; Penzien 2000; Hashash et al. 2001; O'Rourke et al. 2001; Konagai 2005; Wang et al. 2009; Li 2012).

The present paper provides a review of the investigations carried out by various researchers with regard to the seismic performance of mountain tunnels. Some prominent cases of damages reported following recent earthquakes are discussed with special emphasis on the observed damage patterns. Moreover, the factors believed to be responsible for the damages have been explained. Based on the damage patterns and the influencing factors, probable mechanisms of seismic damage of mountain tunnels have been summarized.

Finally, numerical investigation is attempted to evaluate influence of some of the prominent parameters on the seismic performance of tunnels in blocky rock mass. In this regard, a discontinuum based numerical approach has been adopted to simulate the blocky nature of the rock mass. Such an approach towards the seismic analysis of tunnels is very promising especially for tunnels in weathered blocky rock mass as most of the investigations reported in literature are either based on continuum or idealized discontinuum approaches. The highlights of the seismic analyses carried out in the study may be pointed out as following.

- Consideration of fractured nature of the rock mass by Voronoi tessellation scheme which is very rare in literature.
- Explicit investigation of seismic response of tunnels considering wide frequency range (1–10 Hz). For this, seismic analyses with harmonic base excitations of different frequencies have been carried out.
- Influence of Peak Horizontal Acceleration (PHA) on the dynamic forces induced in the tunnel liner has been investigated. This observation has also been correlated with the damages observed in the past case histories viz. 1999 Chi-Chi and 2008 Wenchuan earthquakes.
- Effect of tunnel depth on the seismic response of tunnels has been investigated. The numerical results have also been corroborated with the past damages.

The present study is believed to advance the current understanding with regard to the seismic performance of mountain tunnels passing through blocky rock mass. This may be helpful for number of tunneling projects coming up for various infrastructural developments especially in mountainous regions.

2 Overview of Past Seismic Performances of Mountain Tunnels

Some of the prominent work documenting seismic damages of tunnels and underground facilities have been carried out by Dowding and Rozen (1978), Owen and Scholl (1980), Sharma and Judd (1991) and Power et al. (1998). Dowding and Rozen (1978) investigated 71 tunnels following earthquakes in America and Japan. Most of the tunnels investigated were part of railway or roadway network with majority of them passing through rocky terrain. Based on analysis of the available data, damages may be grouped as damages due to slope instabilities, damages related to poor geology and damages at shallow overburden sections arising due to unsymmetrical loading condition. Damage patterns included uplift of invert, spalling of concrete at the crown, failures of sidewalls and portal cracking. Relationship between seismic damage and peak ground acceleration was established and it was observed that major damages occurred in case of seismic events having a peak acceleration magnitude greater than 0.50 g. The database was further enlarged by Owen and Scholl (1980) documenting 127 cases of damages of underground facilities.

Subsequently, Sharma and Judd (1991) documented 192 cases of tunnel performance under 85 different earthquakes. Correlation of seismic induced damages was made with six parameters: tunnel overburden, type of subsoil, peak ground acceleration, magnitude of earthquake, epicentral distance and type of lining support. It was concluded that the vulnerability of tunnels increased when the depth of overburden was small. Moreover, earthquake parameters like magnitude, peak ground acceleration and epicentral distance had a significant impact on the overall

stability. It was also found that the damage levels decreased for tunnels constructed in competent rocks. Similar observations were made by Power et al. (1998) with regard to the performance of underground facilities following the 1995 Hyogoken-Nanbu (Japan) and the 1995 Northridge (U.S.) earthquakes. Table 1 collates past seismic performances of tunnels highlighting the major observations and conclusions.

3 Specific Discussion on Major Damages

In the present section, case histories of damages of mountain tunnels for earthquakes in Japan, Taiwan and China are discussed. For each of the cases, discussions are made with emphasis on the earthquake parameters, ground conditions and damage patterns documented by various researchers. Based on these case histories, predominant damage patterns and the factors affecting the seismic behaviour of tunnels have been identified.

3.1 Damage of Tunnels in Japan

Owing to the mountainous terrain of Japan, there is an extensive use of tunnels for highway and railway networks. A total of about 4500 tunnels for railways and 6500 tunnels for highways are in operation. In addition, tunnels and underground facilities are also utilized for hydroelectric projects, water supply and storage purpose.

As Japan is situated in a volcanic zone on the Pacific ring of fire, volcanic and earthquake events are quite frequent. Motions arising as a result of movement of Pacific, Philippine, Eurasian and the North American plates results in around 40 earthquake events of magnitude greater than 4.0 per month. As such, seismic damages of tunnel have been reported extensively. Table 2 summarizes cases of tunnel damages following various earthquakes in Japan. Subsequently, some of the major tunnel damages during few prominent earthquakes are discussed.

1923 Kanto earthquake The catastrophic event of Kanto in 1923 caused severe damages to mountain tunnels in Japan. Over 100 cases of tunnel damages were reported following the earthquake out of which 25 needed immediate repair and reinforcement measures. One of the most severely affected tunnel was the Nabuya tunnel which suffered damage from landslide. The landslide destroyed a portion of the tunnel lining leading to collapse of a tunnel section making it inoperative.

1930 Kita-Izu earthquake The 1930 Kita-Izu earthquake of magnitude 7.1 severely affected the Tanna railway tunnel. The earthquake had a focal depth of 11 km. The tunnel was situated at an epicentral distance of 15 km (Sharma and Judd 1991). The damages were maximum in the sections where the tunnel passed through the fault-fracture zone of the Tanna basin. A 60 m stretch of the tunnel without concrete cover was subjected to large earth pressure during seismic shaking. Consequently, large volume of earth (about 1200 m^3) fell into the tunnel disrupting the operations. Cracking of the tunnel lining was also observed at other sections.

1978 Izu-Oshima-Kinkai earthquake This earthquake severely affected the railway network of the adjacent area as it caused extensive damages to nine railway tunnels (Kawakami 1984). Among them, the most severely affected was the Inatori tunnel which was a 906 m long single track railway tunnel passing through a deposit of volcanic mudflow. The damage was majorly caused due to movement along a fault resulting in damage of tunnel lining and distortion of track alignment along the longitudinal direction. Based on the survey conducted following the earthquake, relative displacement of 70 and 20 cm in the horizontal and vertical direction respectively was worked out.

1995 Hyogoken-Nanbu earthquake Asakura and Sato (1998) investigated 100 mountain tunnels following the 1995 Hyogoken-Nanbu earthquake and found that 24 tunnels were affected by the earthquake with 12 of them sustaining heavy damages. In most cases, damages occurred in the form of cracking of the linings in longitudinal, cross-sectional and circumferential direction highlighting the influence of interaction of the direction of seismic waves with the tunnel axis and cross-section. Shear and compressive failure of the sidewalls and the arch, heaving of the invert, cracking of the portal wall and collapse of portal sections were also reported (Asakura and Sato 1998; Kitagawa and Hiraishi 2004). Table 3 summarizes the observations of four most severely affected tunnels following this earthquake.

In case of *Nunobiki tunnel,* cracking in the lining both in the cross-sectional and longitudinal directions were observed. In addition, spalling of concrete at the

Table 1 Past seismic performances of tunnels

References	Main event(s)	Observations	Major conclusions
Dowding and Rozen (1978)	San Francisco (1906) Kwanto (1923) Idu Peninsula (1930) Fukui (1948) Off Tokachi (1952) Kern County (1952) Niigata (1964) Great Alaska (1964)	Caving in of rock near roof and arch shoulder Upward heaving of invert Spalling of concrete at crown Crushing of bottom sidewalls Cracking at portal sections	71 tunnels investigated following earthquake with classification into three categories based on observations—no damage, minor damage and damage Damages are related to peak ground motions No damage observed for ground motion of up to 0.19 g. Minor damage observed in the range of 0.25–0.5 g. Major damage observed for the high peak values of above 0.5 g Damage classified into three categories a. Damage near portals due to slope instability b. Damage in poor ground conditions c. Damage due to shallow depth and unsymmetrical load
Brown et al. (1981)	San Francisco (1906)	Lateral movement of 80 mm of Bay Area Rapid Transit (BART) tunnels at Hayward Fault	Fault movement is a very prominent factor in damaging a tunnel
Murano and Takewaki (1984)	Kanto (1923) Kita-Mino (1961) Izu-Oshima-Kinkai (1978)	Damages to tunnels and powerhouses in rocks especially in portal regions. Longitudinal and transverse cracks in lining observed frequently	Tunnel portals highly vulnerable Poor geology and inadequate lining thickness lead to higher damages Intersection of tunnel with faults should be avoided Amplification of seismic waves in weathered zones increases the vulnerability of portal sections
Yoshikawa (1981); Yoshikawa and Fukuchi (1984)	Kanto (1923) Kitaizu (1930) Fukui (1948) Niigata (1964) Izu-Oshima-Kinkai (1978)	53 cases of heavy damages reported	Damages caused due to poor geology, unstable slopes, fault movement and inadequate lining
Sharma and Judd (1991)	192 cases from 85 earthquakes around the world	Shallow tunnels more prone to seismic damages Greater number of damages for higher peak ground acceleration and smaller epicentral distance Lower damage for tunnels in competent rocks	Damages have been correlated to earthquake parameters, depth and geology

Table 1 continued

References	Main event(s)	Observations	Major conclusions
Asakura and Sato (1996, 1998)	Hyogoken-Nanbu (1995) Kanto (1923) Kita-Tango (1927) Kita-Izu (1930) Fukui (1948) Tokachi-oki (1952) Kita-Mino (1961) Niigata (1964) Tokachi-oki (1968) Izu-Oshima-Kinkai (1978) Miyagiken-oki (1978) Urakawa-oki (1982) Nihonkai-chubu (1983) Naganoken-seibu (1984) Chibaken-toho-oki (1987) Notohanto-oki (1993) Hokkaido-nansei-oki (1993) Hyogoken-Nanbu (1995)	Cracking of lining in longitudinal, cross-sectional and circumferential directions Shear and compressive failure at arch shoulders and sidewalls Heaving and cracking of tunnel invert Cracks at the portal wall Partial/complete collapse of portal region	Majority failure confined to sections located in highly faulted/fractured zone Adverse geological conditions, shallow overburden depth and relative displacement of ground led to failures
Power et al. (1998)	Hyogoken-Nanbu (1995) Northridge (1995) Loma Prieta (1989)	Cracking and spalling damages reported Tunnels with liner performed better during earthquakes Damages can be correlated to peak ground acceleration	PGA < 0.2 g—minor damages 0.2 g $<$ PGA < 0.6 g—Slight to heavy damage Heavy damage in case of 1923 Kanto earthquake majorly caused by slope instabilities and shallow overburden
Wang et al. (2001)	Chi-Chi (1999)	Damage to unreinforced secondary lining Longitudinal, circumferential and inclined cracking Cave in and collapse at shallow overburden (35–45 m) sections Support damage due to squeezing ground for deeper sections (>100 m)	The unreinforced secondary lining suffered damages due to excessive earthquake loading Imperfect backfill, bad geometry of tunnel cross section and poor geological conditions contributed to damage Maximum damage in the region passing through Sanyi and Shihliufen fault having shallow overburden highlights the effects of adverse geology and depth of tunnel section from ground

Table 2 Summary of tunnel damages following earthquakes in Japan. (Adapted from Asakura and Sato 1998; Otsuka et al. 1997)

Earthquake	Magnitude	Tunnel performance
Kanto (1923)	7.9	Severe damages to over 100 tunnels. Damages caused due to fault intersection, slope instabilities and debris flow
Kita-Tango (1927)	7.3	Minor damage to two railway tunnels
Kita-Izu (1930)	7.3	Severe damage arising from fault intersection and movement reported for one railway tunnel
Fukui (1948)	7.1	Severe damage to two railway tunnels
Tokachi-oki (1952)	8.2	10 railway tunnels damaged slightly
Niigata (1964)	7.5	Severe damages to 20 railway tunnels and one road tunnel. Damages occurred due to poor geological conditions and subsequent landslides in the form of cracking of tunnel lining
Tokachi-Oki (1968)	7.9	Damages to 23 railway tunnels. Constant landslides and increased earth pressure responsible for damages
Izu-Oshima-Kinkai (1978)	7.0	Very severe damages to about 9 railway and 4 road tunnels. Damages attributed to poor geological conditions, fault crossing and rock falls
Miyagiken-oki (1978)	7.4	Slight damage to 6 railway tunnels located near epicentre
Urakawa-oki (1982)	7.1	Slight damage to 6 railway tunnels
Nihonkai-chubu (1983)	7.7	Slight damage to 8 railway tunnels
Naganoken-seibu (1984)	6.8	Cracking observed in one head race tunnel majorly caused due to fault crossing
Chibaken-toho-oki (1987)	6.7	Damage to a railway tunnel
Notohanto-oki (1993)	6.6	Severe damage to a rock tunnel due to collapse of rock onto the tunnel lining
Hokkaido-nansei-oki (1993)	7.8	Rock fall induced failure at portal sections for one road tunnel

Table 3 Summary of few tunnels damaged in 1995 Hyogoken-Nanbu earthquake. (Adapted from Asakura and Sato 1998; Otsuka et al. 1997)

Tunnel	Overburden (m)	Geology	Epicentral distance (km)	Damages observed
Maiko	4–50	Granite, sand-gravel	5	Settlement of crown, exfoliation and cracking of shotcrete
Nunobiki	240	Mesozoic granite	18	Exfoliation of concrete lining, development of ring cracks
Bantaki	20–250	Mesozoic granite	32	Exfoliation of concrete lining, development of ring cracks
Rokko	0–400	Mesozoic granite	20–30	Damage at 12 locations near fractured zones, heave of invert, shear failure and cracking of lining

junction between the arch and the sidewall was also observed. However, the damage was confined to a short zone which was comparatively heavily fractured.

The damages in the case of *Bantaki* road tunnel was also confined to a short section of highly fractured zone characterized by buckling and bending of steel reinforcements. In addition, strong vertical ground motions and thrusting in the axial direction were held responsible for the uplift of the ground pavement.

The *Rokko* tunnel was a 16 km long railway tunnel constructed in Mesozoic granite with the alignment passing thorough five major faults—Koyo, Ashiya, Gosukebashi, Ohtsaki and Nunobiki faults. The poor geological condition arising from the frequent faulting and fracturing led to different configurations of failures. Some prominent patterns of failures observed included the development of shear cracks and spalling of concrete near the arch shoulders. Bottom heaving

and uplift in the vicinity of the inverts were also reported. Major damages occurred in the poor and highly fractured geological zone encountered between the Gosukebashi and Ohtsaki faults.

One of the main factors leading to failures was the adverse geology associated with the damaged tunnel sections. This clearly highlights the adverse effects of discontinuities leading to amplified ground motion and relative movements among rock blocks (Roy and Sarkar 2015). Some of the other factors influencing the magnitude of relative displacement among blocks are degree of separation, direction of ground motion and topography.

2004 Mid-Niigata Prefecture earthquake The earthquake occurred on October 23, 2004 severely affecting the rail and road network of the area. The focal depth of the earthquake was about 13 km having a magnitude of 6.8. A series of strong aftershocks followed the main events with four of them having a magnitude of around 6 or greater in a span of 38 min (Konagai et al. 2005). The earthquake affected about 24 railway tunnels and even caused the derailment of a train. Among them, five tunnels—Uonama, Myoken, Wanatsu, Tenno and Shin-Enokitoge suffered severe damages and had to be closed for a long time for repair and restoration (Shimizu et al. 2007b, Yashiro and Kojima 2007; Jiang et al. 2010).

The Uonama tunnel located close to the epicenter (<10 km) suffered maximum damage. The damaged section had an overburden of about 60–100 m. Movement of sidewalls along with development of diagonal cracks was common. At one location, severe damage at the crown leading to lining collapse and exposure of steel reinforcements was observed. As shown in Fig. 1, right lateral shift of about 10–15 cm

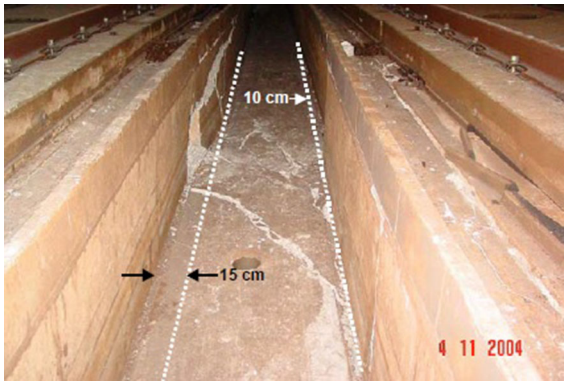

Fig. 1 Right lateral shift of about 10–15 cm in Uonama tunnel (Konagai et al. 2005)

of the center ditch along the rails was also observed (Konagai et al. 2005).

Even though landslide was prevalent during the earthquake, it is believed that it was not the major cause as the damaged sections were located at deeper depths. Based on the pattern of cracks observed, it has been concluded that the damage was caused by slipping of a fault segment intersecting the tunnel.

Another tunnel to be severely affected was Myoken tunnel. Failures in terms of heaving of the invert and compressive failure at the crown were observed. In case of Wanatsu tunnel, compressive failure at crown with subsequent exposure of steel supports was observed. For both Tenno and Shin-Enokitoge tunnels, cracking of tunnel lining resulting from failure of bedrock was reported (Shimizu et al. 2007b, Jiang et al. 2010). A list of tunnels affected by the earthquake along with the associated geology and damage patterns has been reproduced from the study of Jiang et al. (2010) in Table 4.

3.2 Damage of Tunnels in Taiwan

1999 Chi-Chi earthquake A 7.3 magnitude earthquake struck central Taiwan on September 21, 1999 at a depth of around 7.5 km causing catastrophic damage to infrastructural facilities. The earthquake is believed to be a result of reactivation of the Chelungpu fault (Wang et al. 2000). The seismic event produced very high ground motion with the free field instruments recording horizontal motion of 1.0 and 0.8 g at two locations (Wang et al. 2001).

Figure 2 shows the location of the tunnels in vicinity of the earthquake epicenter and the Chelungpu fault. Following the earthquake, an investigation of 57 tunnels was taken up by Wang et al. (2001) based on which 49 cases of damages were reported. Figure 3 presents number of different damage patterns observed in case of reported 49 cases of instabilities. From the figure it is evident that the damages of tunnel sections are mostly in forms of lining cracks, portal failure and spalling of concrete lining. Figure 4 shows the slope instability induced failure of the Ching-Shue tunnel following this earthquake.

Table 5 reproduced from Wang et al. (2001) lists the 57 tunnels which were investigated providing details about their geometry, epicentral distance and location with regard to the Chelungpu fault. Greater damages were observed for tunnels located on the

Table 4 Tunnels damaged in Mid-Niigata Prefecture earthquake (After Jiang et al. 2010)

Tunnel	Length (m)	Overburden (m)	Width (m)	Height (m)	Geology	Damages
Wanatu	300	40	8.2	4.6	Ss	Side wall deformation and spalling of arch
Kosendani	1088	62	9.5	4.8	Ss	Crack, spalling in arch and sidewall
Yamamotoyama	1839	140	10.2	7.5	Absm	Crack
Yamanaka	1307	200	6.5	4.5	Ss, Ms	Longitudinal crack
Takeisi	331	140	7	7.74	Ss, Ms	Longitudinal crack
Higasiyama	220	35	7	4.7	Ss, Ms	Crack in arch
Siroyama	128	150	7	4.7	Ss, Ms	Longitudinal crack in sidewall
Orinaka	374	60	9.25	4.7	Ss, Ms	Crack in arch and sidewall
Obirou	390	90	9.25	4.7	Ss, Ms	Crack
Sibumi	860	150	6	4.7	An, Tu, Ms	Spalling in arch
Haneguro (roadway)	506	100	5.6	5.2	St	Compressive buckling in bed, crack in arch and sidewall
Haneguro (pavement)	550	100	2.2	2.85	St	Spalling
Junidaira	210	40	8.5	4.7	St	Spalling, deformation in sidewall
Rangi	590	180	6	4.7	Ss, Ms	Longitudinal crack in arch, upheave in bed
Siotani	512.5	110	7.5	5.85	Ss, Ms	Crack in arch
Kizawa	305	30	6	4.7	Ss, Ms	Deformation, spalling, roadbed opening
Araya	292	45	7.5	5.64	Ss, Ms	Compressive buckling, crack, bed opening
Tochio	854	150	10.35	4.7	An, Ms	Water leakage
Okimitouge	1080	150	8.5	4.7	Ms, Ss	Longitudinal crack in sidewall
Hosa	6087	15	9.6	8.3	Tb	Crack in roadbed
Horinouti	3300	100	9.6	8.3	Cm	Spalling in sidewall
Uonama	8624	70	9.6	8.3	Ms, Absm	Spalling, upheave in bed, crack
Myoken	1459	65	9.6	8.3	St	Crack, upheave in roadbed
Takitani	2673	55	9.6	8.3	St, Ss	Crack
Sinfukuyama	1468	75	4.8	5	Sr	Crack
Fukuyama	1350	7	4.8	5.6	Sr	Crack
Wanatu	725	41	8.5	7.5	St	Spalling, crack, arch-shoulder junction failure
Nakayama	1205	92	8.5	7.5	Sh, Ss	Crack
Usigazima	432	14	8.5	7.5	Sh, Ss	Crack in portal
Tenou	285	11	4.7	5.1	Sh, Ss	Crack
Sintouge	1372	75	4.7	5.1	Sh, Ss	Crack
Touge	641	70	4.8	5.1	Sh, Ss	Crack
Hanada	880	28	8.6	6.3	Sh, Ss	Spalling
Tukayama	1766	150	8.7	6.3	Sh, Ss	Crack
Higasiyama	166	22	8.8	6.4	Ms, Ss	Spalling
Iwayama	652	54	4.7	5.2	Ss	Spalling
Iwazama	203	36	4.6	5.1	St	Spalling
Myokouzan	1465	151	4.6	5.2	Ar	Crack

Table 4 continued

Tunnel	Length (m)	Overburden (m)	Width (m)	Height (m)	Geology	Damages
Kouyouzan	500	67	4.8	5.1	Sr	Crack
Utigamaki	425	30	4.6	5.2	Ms	Crack
Akakura	10,471	440	4.36–8.54	6.16–6.96	Ms, Ss	Spalling, crack in arch and sidewall, water leakage
Jusanmachi	1695	40	5.05	5.68	Cm	Water leakage
Yakusitoge	6199	250	4.36–8.54	5.60–6.96	Ms	Spalling, crack in arch and sidewall, water leakage

Ss sandstone, *Absm* alternating beds of sandstone and mudstone, *Ms* mudstone, *An* andesite, *Tu* tuff, *St* siltstone, *Tb* tuff breccias, *Cm* conglomerate, *Sh* shale

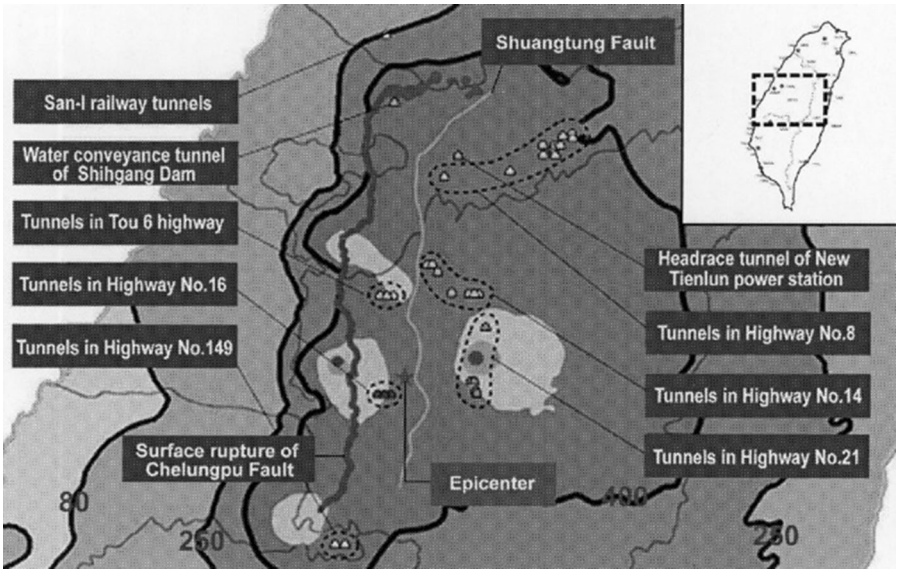

Fig. 2 Location of tunnels and Chelungpu Fault in vicinity of epicenter of Chi-Chi earthquake (Wang et al. 2001)

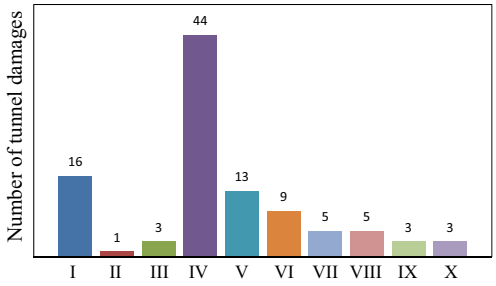

I: Portal failure II: Sheared off lining III: Slope induced failure IV: Lining cracks V: Concrete spalling VI: Water inrush VII: Exposed reinforcement VIII: Displaced lining IX: Pavement cracks X: Rock falls in unlined section

Fig. 3 Various tunnel damages observed in Chi-Chi (1999) Taiwan earthquake

hanging wall of the Chelungpu fault which experienced higher ground motion. It was observed that the damages are mainly concentrated in the vicinity of the faulted or fractured region.

3.3 Damage of Tunnels in China

2008 Wenchuan earthquake On May 12, 2008 a strong earthquake having a magnitude of 8.0 on Richter scale struck in the Longmenshan fault zone in the Sinchuan Province of China (Chen et al. 2012; Huang and Li 2009; Xu et al. 2009). The focal depth of the earthquake was estimated to be around 15 km with

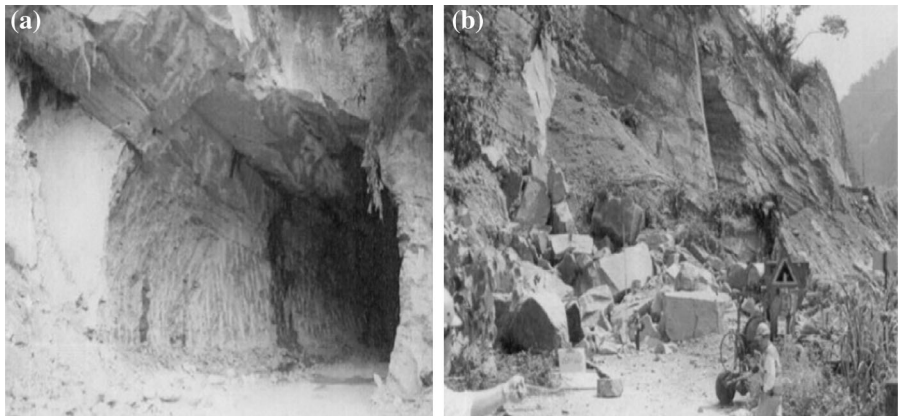

Fig. 4 Damage to Ching-Shue tunnel. **a** Tunnel entrance before the Chi-Chi earthquake. **b** Closure and damage of tunnel entrance due to slope instability (Wang et al. 2001)

the seismic shaking period of 120 s. This earthquake is believed to be the most destructive seismic event to have struck China in the last 100 years affecting around 87,000 people and causing an economic loss of about 845 billion Yuan. Table 6 lists 30 tunnels having an epicentral distance less than 50 km which suffered damages during the earthquake (Wang and Zhang 2013; Zhang 2013; Zheng et al. 2009, 2012).

Li (2012) has carried out a more detailed investigation of the damages to the mountain tunnels of the Dujiangyan Wenchuan highway tunnels following the Wenchuan earthquake highlighting the damage patterns and the factors contributing towards the instabilities. Table 7 summarizes the findings of Li (2012) with regard to 11 tunnels of the Du Wen highway network which were affected by the earthquake. Details of some of the damaged tunnels are elaborately discussed in the following section.

Longxi tunnel It is a twin tunnel system separated by a distance of 30 m. According to the rock mass classification system of Chinese highway tunnel, the alignment passes though two zones. About 29 % of the tunnel length passes through sandstone and granite rock which is hard and hence has good overall stability. However, 71 % tunnel passes through intensely jointed and fractured rock mass comprising of mudstone, mudstone-siltstone mixture, carbonaceous mudstone and thin coal layers. In such stretches the stability was poor. Following the earthquake, instabilities were manifested in terms of portal closure, cracking of pavement and tunnel linings (Li 2012; Chen et al. 2012; Shen et al. 2014).

Due to high and steep configuration of slope, rock falls obstructed the tunnel entrance and destroyed the slope protection works. Figure 5a shows a rock block which fell across the opening during the earthquake. Moreover, five cases of collapse of lining due to presence of weak mudstone at entrance sections were observed (Li 2012). The tunnel linings were sheared off at some locations as shown in Fig. 5b. In addition, transverse ring cracks as shown in Fig. 5c developed in a particular stretch of the tunnel. A maximum ground bulge of about 120 cm with heaving and bulging of tunnel invert was also observed. Figure 5d shows the cracks which developed at the pavement as a result of uplift of the bottom pavement.

Baiyunding tunnel The tunnel has a maximum overburden of 125 m and passes through limestone formation which is highly weathered. Intense fracturing in the area filled with moist and loose gravel soil has lead to poor quality of rock mass. A fault belt also exists about 45 m away from one of the portals intersecting the tunnel axis. During the Wenchuan earthquake, widespread damage was reported at the portal sections resulting from a landslide as shown in Fig. 6a. Settlement of basement, cracking of the flooring and an average dislocation of around 20 cm was noted for a damage length of about 30 m leading to an adverse impact on the functionality of the tunnel (Chen et al. 2012). Moreover, spalling of concrete lining and shearing failure was also observed at number of sections. Figure 6b shows a section where the reinforcement was exposed as a result of shearing off and spalling of concrete liner.

Table 5 Tunnel investigated following the 1999 Chi-Chi earthquake (after Wang et al. 2001)

Tunnel and location	Length (m)	Width (m)	Distance to epicentre (km)	Distance to Chelungpu fault (km)
Shih-Gang Dam, Water conveyance tunnel	–	–	–	0.0
Highway 8, 13 k + 381	20	6.5	35.1	12.0
Highway 8, 27 k + 710, Li Lang	30	6.8	38.6	18.6
Highway 8, 34 k + 668	50	3.2	44.0	20.1
Highway 8, 34 k + 775	41	3.4	44.0	20.1
Highway 8, 35 k + 908, Old Ku-Kuan	90	5.1	44.8	19.8
Highway 8, 36 k + 908, Ku-Kuan	90	7.5	44.8	19.8
Highway 8, 38 k + 500, No. 1 old Maa-Ling	150	4.0	45.9	21.5
Highway 8, 38 k + 500, No. 1 Maa-Ling	365	5.1	45.8	21.5
Highway 8, 39 k + 075, No. 2 Maa-Ling	60	7.5	46.1	21.6
Highway 8, 40 k + 830, No. 3 Maa-Ling	245	7.5	46.3	21.6
Highway 8, 41 k + 311, No. 4 Maa-Ling	100	7.5	47.8	22.1
Highway 8, 41 k + 311, No. 4 old Maa-Ling	100	4.0	47.8	22.1
Highway 8, 42 k + 573	10	6.5	48.3	23.0
Highway 8, 43 k + 040	15	6.5	48.3	23.0
Highway 8, 45 k + 266	32	6.5	48.5	22.8
Highway 14, 37 k + 405, Shuang-Fu	150	7.5	19.7	12.0
Highway 14, 37 k + 981(L), Gang-Lin	182	7.5	19.8	12.2
Highway 14, 38 k + 000(R), Gang-Lin	249	7.5	19.8	12.2
Highway 14, 39 k + 921(L), Yu-Ler	158	7.5	19.0	13.8
Highway 14, 39 k + 921(R), Yu-Ler	158	7.5	19.0	13.8
Highway 14, 45 k + 182, Pei-Shan	120	7.5	15.9	17.5
Highway 14, 48 k + 616(L), No. 1 Kuan-Yin	129	7.5	17.1	20.4
Highway 14, 48 k + 616(R), No. 1 Kuan-Yin	129	7.5	17.1	20.4
Highway 14, 48 k + 787(L), No. 2 Kuan-Yin	123	7.5	17.5	20.8
Highway 14, 48 k + 787(R), No. 2 Kuan-Yin	123	7.5	17.5	20.8
Highway 14, 49 k + 253(L), No. 3 Kuan-Yin	252	7.5	17.6	21.2
Highway 14, 49 k + 253(R), No. 3 Kuan-Yin	252	7.5	17.6	21.2
Hghway 16, Chi-Chi	238	4.8	6.1	5.5
Highway 16, New Chi-Chi (L)	580	7.5	6.4	5.3
Highway 16, New Chi-Chi (R)	515	7.5	6.4	5.3
Highway 21, 54 k + 326 (L), Da-Yuan	462	7.5	14.2	21.8
Highway 21, 54 k + 326 (R), Da-Yuan	444	7.5	14.2	21.8
Highway 21, 66 k + 940 (L), Shue-Sir	185	7.5	8.5	19.9
Highway 21, 66 k + 940 (R), Shue-Sir	185	7.5	8.5	19.9
Highway 21A, 17 k + 303, No. 1 Huan-Hu	128	7.5	9.3	20.2
Highway 21A, 17 k + 253, No. 2 Huan-Hu	61	7.5	9.3	20.2
Highway 149, Tsao-Ling	505	7.0	31.1	7.0
Highway 149, Ching-Shue	52	7.5	32.0	3.7
Tou-6 highway, No. 1 Tu-Cheng	100	6.5	15.5	7.2
Tou-6 highway, No. 2 Tu-Cheng	290	6.4	15.3	7.6
Tou-6 highway, Shuang-Lung (E)	140	5.3	15.2	7.8
Tou-6 highway, Shuan-Lung (W)	90	5.3	15.2	7.8

Table 5 continued

Tunnel and location	Length (m)	Width (m)	Distance to epicentre (km)	Distance to Chelungpu fault (km)
Tou-6 highway, No. 1 Shuang-Tung	80	4.5	15.2	7.8
Tou-6 highway, No. 2 Shuang-Tung	120	4.5	15.2	7.8
Chi-Chi line railway, No. 1 tunnel	350	5.0	6.1	5.5
Chi-Chi line railway, No. 2 tunnel	1400	5.0	<1	11
Chi-Chi line railway, No. 3 tunnel	250	5.0	4.5	15.9
Chi-Chi line railway, No. 5 tunnel	150	5.0	5.5	16.4
Da-Kuan power station, headrace tunnel	–	–	8.5	19.9
New Tien-Lun power station, headrace tunnel	10,600	5.0	40	18.6
Mountain line railway, No. 1 San-I tunnel	7540	9.1	55	11.1
Mountain line railway, No. 2 San-I tunnel	260	9.1	50	10.1
Mountain line railway, No. 3 San-I tunnel	520	9.1	49	10.1
Mountain line railway, No. 4 San-I tunnel	455	9.1	49	10.1
Old mountain line railway, No. 1 San-I tunnel	230	5.0	59	14.5
Old mountain line railway, No. 2 San-I tunnel	730	5.0	58	13.1

Longchi tunnel The tunnel passes through limestone formation having a maximum overburden depth of 345 m. However, the terrain becomes steep at the portal regions with an overburden of about 50 m. Intense weathering of rock mass and presence of faults near portals contributed adversely during the earthquake leading to failures. Cracking of tunnel lining in transverse, longitudinal and inclined directions as shown in Fig. 7a, b were noted. Moreover, the cracking and undulation of the bottom pavement was also observed.

Youyi tunnel It is a 962 m long tunnel having maximum overburden of 215 m with flat terrains at the portal ends. The tunnel passes through carbonaceous shale, argillaceous shale and sandstone with the portal sections located in gravelly soil. Relative movement along the faults caused tunnel liner to be sheared off along with deformation and cracks. Subsequent landslide induced failure at the portal sections. Figure 8a shows a damaged portal section near one of the tunnel entrance. The exposure of reinforcements as a result of spalling of tunnel lining is shown in Fig. 8b.

Shen et al. (2014) compiled the seismic response of 52 tunnels following the 2008 Wenchuan earthquake classifying the observed damage patterns into eight categories. Based on the data, Fig. 9 presents number of different damage patterns observed following the seismic event. From the figure it is evident that the damages of tunnel sections are mostly in forms of lining cracks and rock falls.

4 Summary of Failure Characteristics

4.1 Cracking of Tunnel Lining

The most frequent form of earthquake induced damages in tunnels is the cracking of the tunnel lining. Based on field observations of tunnel damages, the cracking have been classified as longitudinal, horizontal, oblique breakage, ring breakage and invert cracks. Figure 10 shows some of the crack patterns generally observed following recent past seismic events. Many tunnels severely damaged in 1923 Great Kanto earthquake developed longitudinal, horizontal and oblique cracks in the lining. Various forms of cracking have also been reported by Li (2012) for the tunnels of the Du Wen highway following the Wenchuan earthquake of 2008. In some cases, cracks developed at both sides of arch wall. Moreover, at some sections, extensive collapse of the concrete lining coupled with the exposure and buckling of steel reinforcements compromised the safe operation of the tunnels.

Table 6 Tunnel with an epicentral distance of less than 50 km in the 2008 Wenchuan earthquake (Wang and Zhang 2013)

Tunnel name	Length (m)	Epicentral distance (km)
Longxi	3624	1.6
Zipingpu	4075	7.3
Longdongzi	1051	5
Shaohuoping	450	4.5
Zaojiaowan	1926	8.9
Maojiaowan	399	11.4
Chediguan	403	13
Futang	2365	13
Taoguan	625	7.9
Caopo	759	34.4
Dankanliangzi	1555	24.1
Maanshi	481	7.3
Youyi	962	2.4
Baiyunding	406	6.5
Panlongshan	381	14
Gengda	938	11.4
Niujiaoya	1614	4
Sanpanzi	382	13.2
Jiujiaya	2282	9.6
Longchi	1177	1.1
Xiquanyan	150	28
Xinjiagou	713	45
Guanyazi	639	43
Fenshuiling	1300	22
Shiwenzi	1300	42
Shitigou	371	43
Qujiapo	601	33
Feixianguan	384	37
Minyuexia	1300	38
Qinglinpo	255	40

4.2 Shear Failure of Tunnel Lining

One of the most severe forms of earthquake damages is the shear failure of the tunnel lining. This type of failure results from the shear force acting on the lining near the faults and is characterized by the spalling of concrete coupled with exposure and detachment of steel reinforcements. The Tanna tunnel in Japan was severely affected by the shearing failure leading to severe cracks at several locations during 1930 Kita-Izu earthquake. For this particular case a horizontal displacement of 2.39 m and a vertical displacement of 0.6 m were observed near the Ena fault zone (Dowding and Rozen 1978).

More recently, the Longxi tunnel was severely affected in the 2008 Wenchuan earthquake and became inoperative following about 1 m up and down relative displacement at some locations leading to the collapse of the arch lining. Severe damages to the secondary lining of the Baiyunding tunnel leading to the loss of structural integrity have also been attributed to the shear failure of the lining.

Although the shearing failure of tunnel lining is generally expected for regions crossing the faults, some damages in tunnels with alignment not crossing the fault have also been reported. Prominent among them is the case of the Nagasaka tunnel which was damaged in the 1923 Great Kanto earthquake (Chen et al. 2012).

4.3 Portal Failure

Review of case histories highlights the fact that the portal sections are the most vulnerable part of the tunnel (Zhao et al. 2013). Instabilities in the form of rock falls, avalanches and sliding, cracking of head walls, arch rings, wing walls and expansion joints are the most noted failures following seismic events.

Rock falls occur in steep slopes consisting of relatively strong and unfractured rock masses. Such damages were observed in case of Longxi tunnel where the rock fall destroyed the slope protection measures (see Fig. 5a). In contrast, sliding failure occurs in vicinity of portal sections where the geological medium consists of highly weathered and fractured rock mass as in the case of the Longdongzi tunnel (Li 2012) during 2008 Wenchuan earthquake. The weathered nature of the geological medium coupled with the steepness of the slope and the presence of unfavorably dipping structural planes led to sliding of the rock material burying the right hand tunnel exit of the Longdongzi tunnel following the Wenchuan earthquake. Spalling and cracking of concrete lining on the arch side wall for the Taoguan tunnel with crack widths reaching up to 50 cm are also attributed to the slope instabilities in the portal region following the earthquake (Li 2012).

Table 7 Tunnels of Du Wen highway affected by 2008 Wenchuan earthquake (after Li 2012; Wang et al. 2009)

Tunnel	Epicenter distance (km)	Adverse impacts
Zipingpu tunnel	50	Transverse and ring fractures of lining, uplift and cracking of invert and partial collapse of portal
Longdongzi tunnel	30	Portal burial, longitudinal cracks (20–35 m long), transverse, oblique and ring cracks with 10–20 mm opening
Longxi tunnel	49	Obstruction of tunnel from rock falls, longitudinal, transverse, oblique and ring fractures of lining, distortion of steel beams, opening of construction joints, uplift of invert up to a maximum height of 1.2 m
Shaohuoping tunnel	40	Collapse of slope leading to portal burial, transverse fracture and uplift of invert, water seepage, distortion of steel supports
Zaojiaowan tunnel	42	Leakage of water through construction joints
Maojiawan tunnel	35	Partial burial of portal due to rock fall, cracking of construction joints in portal sections
Chediguan tunnel	32	Partial burial of portal, development of ring cracks at portal sections, cracking of road bed
Futang tunnel	45	Oblique cracks (45°) in entrance section extending to 30 m, seepage of water through construction joints
Taoguan tunnel	28	Partial burial of portal section due to rock falls
Caopo tunnel	25	Rock falls at portal regions, water seepage through side wall cracks
Dankanliangzi tunnel	10	Minor cracking at portal section

Fig. 5 Damages at Longxi tunnel during 2008 Wenchuan earthquake (modified after Tao et al. 2011): **a** Rockfall causing obstruction at tunnel entrance, **b** sheared off tunnel lining, **c** transverse ring cracks, **d** pavement cracks due to uplift

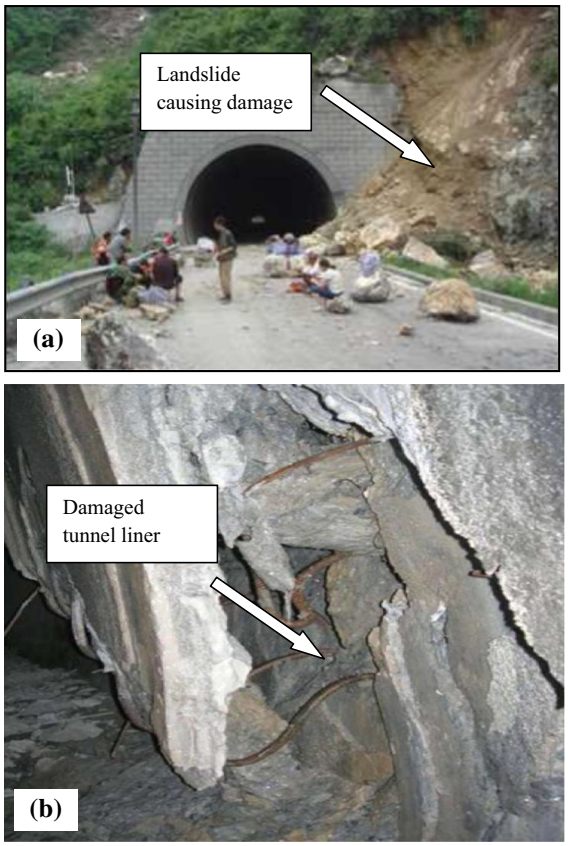

Fig. 6 Damages at Baiyunding tunnel (modified after Tao et al. 2011): **a** portal section damage due to landslide, **b** sheared off tunnel liner

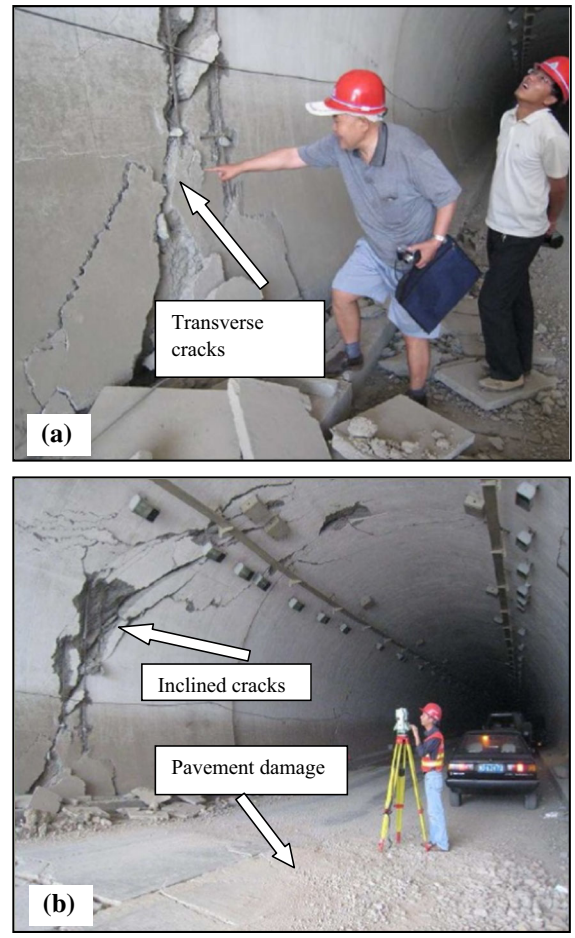

Fig. 7 Damages at Longchi tunnel (modified after Tao et al. 2011): **a** transverse cracking of liner, **b** inclined cracks and pavement damage

4.4 Heaving and Cracking of Tunnel Invert

A number of cases of heaving and cracking of tunnel invert has been reported (Shen et al. 2014; Duke and Leeds 1959). A typical characteristic of this type of failure is the development of transverse cracks. In case of the Longxi tunnel, deformations in both the horizontal and vertical directions of about 30 cm were noted. Also, a maximum uplift of 120 cm was reported in one of the sections (Shen et al. 2014). Following the 1923 Great Kanto earthquake, Namutani tunnel suffered enormous lining distortion due to the uplift of the bottom slab. The displacement ranged between 50 cm and 1 m along the axis of the tunnel (Duke and Leeds 1959). In case of Longdongzi tunnel also, an uplift of about of 2 cm was observed (Li 2012).

From a number of case studies, it was concluded that the uplift and cracking of tunnel inverts were more predominant in case of presence of center drainage. This is attributed to the concentration of shear force and stiffness mismatch near the tunnel invert. In addition, the abrupt changes in the cross section at the invert leading to stress concentration is also regarded as a cause for such damages (Shen et al. 2014).

5 Factors Affecting Mountain Tunnel Damage

5.1 Earthquake Parameters

The major earthquake parameters causing seismic damages of mountain tunnels include magnitude, epicentral distance and the depth of the earthquake source. In conjunction, the three major parameters define the severity of a seismic event. Any earthquake

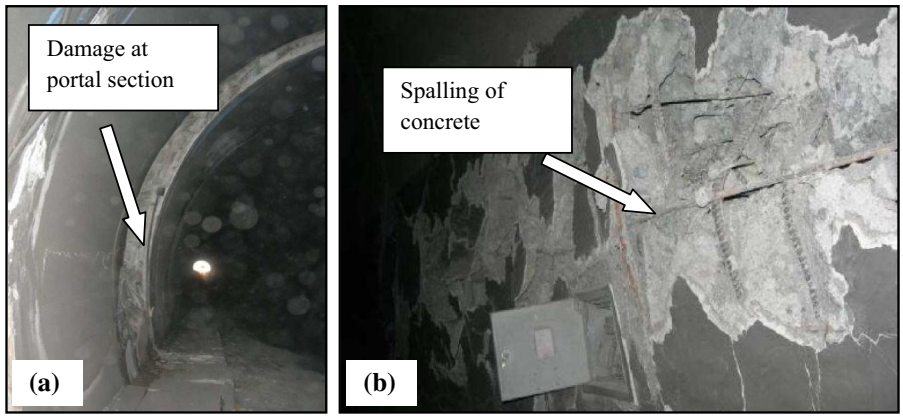

Fig. 8 Damages at Youyi tunnel (modified after Tao et al. 2011): **a** damage at portal section, **b** spalling of concrete from tunnel lining

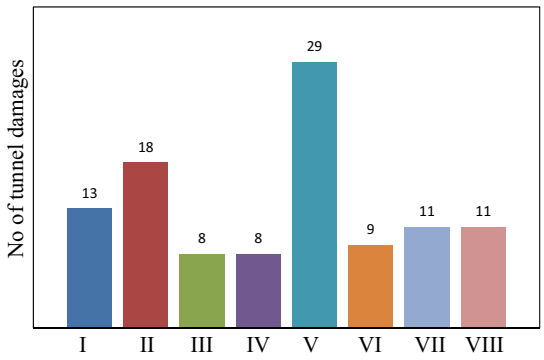

Fig. 9 Various tunnel damages observed in Wenchuan (2008) China earthquake

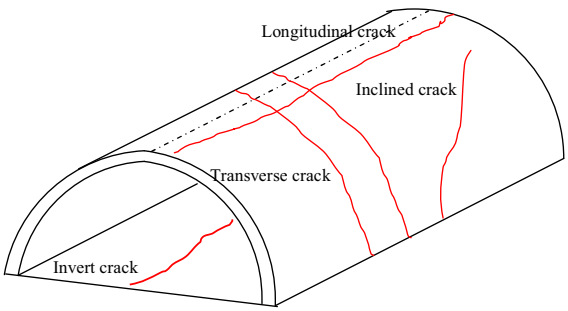

Fig. 10 Different patterns of cracks in tunnel lining

having a higher magnitude, lower epicentral distance and a shallower depth will be more intense and influence the tunnels to a greater extent.

Sharma and Judd (1991) collected and analyzed data for 192 tunnels from 85 different earthquakes based on which the influence of magnitude and epicentral distance on the seismic performances were summarized. Table 8 summarizes the effect of Richter magnitude on tunnel damages. It was observed that the number of cases of tunnel damage reaches about 50 % for magnitudes greater than 6.0. At lower magnitudes, the number of cases of damages was low. Recent damages of mountain tunnels reported in literature following 1999 Chi-Chi, 2004 Mid-Niigata Prefecture and 2008 Wenchuan earthquakes also conform to these findings with most of the damages associated with magnitude greater than 6.0 on the Richter scale (Wang et al. 2001; Shen et al. 2014; Shimizu et al. 2007a, b; Jiang et al. 2010).

Table 8 Summary relating damage with Richter magnitude (after Sharma and Judd 1991)

Magnitude	Extent of damage			
	Slight	Moderate	Heavy	None
<4	2	1	1	3
4–<5	1	2	0	8
5–<6	2	2	1	12
6–<7	17	3	6	33
7–<8	13	8	6	17
>8	10	7	6	22

With consideration to the epicentral distance, it is observed that the seismic vulnerability of the tunnels increases when they are situated closure to the source of the earthquake. In most of the reviewed cases, it has been found that the epicentral distance for the damaged tunnels was within 70 km (Asakura and Sato 1998; Otsuka et al. 1997; Wang et al. 2001). Table 9 summarizes the findings of Sharma and Judd (1991)

Table 9 Summary relating damage with epicentral distance (After Sharma and Judd 1991)

Epicentral distance (km)	Extent of damage			
	Slight	Moderate	Heavy	None
<25	30	13	7	20
25–<50	2	7	8	25
50–<100	10	1	2	26
100–<150	2	1	1	9
150–<200	1	0	0	6
200–<300	0	0	0	3

relating tunnel damages with epicentral distance. However, review of recent case studies does not strictly conform to these observations. In some cases, tunnels located farther away (about 40 km) suffered greater damages in comparison to those located close to the earthquake source (Chen et al. 2012).

5.2 Overburden Depth

Sharma and Judd (1991) analyzed the effect of depth of overburden for 132 cases and concluded that overburden plays major role in influencing tunnel damages. Based on the analysis of available data, they concluded that the damages are more with the tunnel depths less than 50 m. However, in contrast, few damages of mountain tunnels show deviation from the above mentioned conclusion. Prominent among these are the damage cases of the Rokko tunnel and the Longxi tunnel. In fact, in the case of the Longxi tunnel, serious damages were observed at a depth of 500 m in terms of collapse of a portion of the secondary concrete lining during 2008 Wenchuan earthquake (Li 2012).

5.3 Fault Location

Permanent ground displacements resulting from fault movements during earthquakes have caused a number of failures of tunnels. In such events, large shear forces act on the tunnel sections and cause relative movement in both horizontal and vertical directions. Some of the prominent cases of fault induced damages include the case of Uonama (2004 Mid-Niigata Prefecture), Inatori (1978 Izu-Oshima-Kinkai) and the Tanna (1930 Kita-Izu) tunnels.

A total of more than 40 tunnel damages related to fault movement have been identified following the 1999 Chi-Chi Taiwan earthquake (Wang et al. 2001; Chen et al. 2012). In addition, fault movements have also caused damages to tunnels situated in vicinity of faults by inducing permanent deformations of the surrounding ground. Such damages have been reported for the Longxi, Longdongzi and Zipingpu tunnels of the Du Wen highway network (Li 2012). Even though these tunnels did not cross the main fault, secondary effects of fault movement of 2008 Wenchuan earthquake led to severe damages. The cases of damages for Shanglongshan, Shaohuoping, Jiujiaya and the Jiangejianmen tunnels during recent earthquakes are also related to ground deformation induced by fault movement.

5.4 Geology

The geological configuration through which the tunnel passes has a very significant impact on its stability during seismic scenario. It is observed that seismic damages of mountain tunnels are concentrated at zones which are weathered and/or fractured. However, tunnel passing through competent rock mass seldom suffer any significant damage (Kumari and Sitharam 2012).

Observation of instabilities at the portal section arising due to rock falls, sliding and collapse have been widely documented. The high vulnerability of portals is attributed to the poor geological conditions and shallow overburden depth.

Generally, the portal sections are located in highly weathered rock formation or relatively loose quaternary deposits. Such ground conditions leads to amplification of seismic waves resulting in higher ground deformations. The increased seismic deformation demand exceeding the tunnel capacity leads to various forms of damages.

Seismic vulnerability also increases when the tunnel passes through a transition zone between hard and soft rocks. For example, in case of Longxi tunnel, greater seismic damage occurred for the portal region situated in mudstone in comparison to the zone passing through granite rock. Figure 11 illustrates the vulnerability of tunnel passing through a transition zone. In such geological condition, mismatch in both stiffness and seismic impedance leads to differential kinematic movement. This kinematic movement coupled with amplified ground motion due to the softer strata results in an additional horizontal force on the tunnel liner leading to the development of cracks at the junction between the arch shoulder and the sidewall as

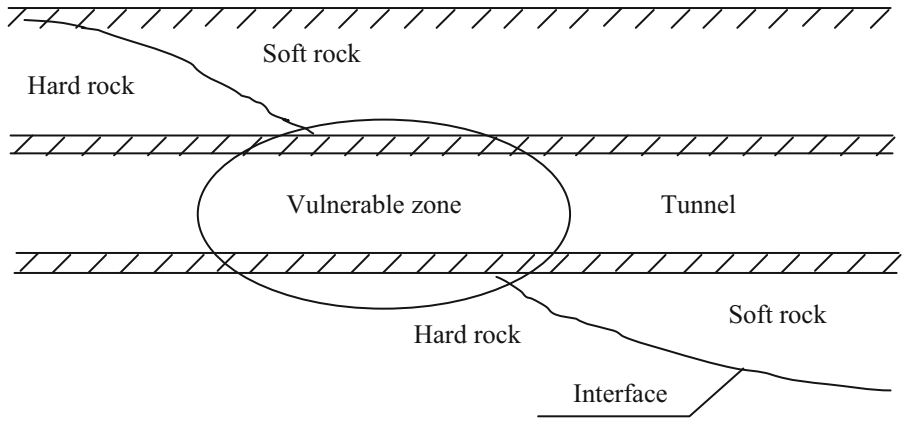

Fig. 11 High vulnerability at interface between two types of rock mass

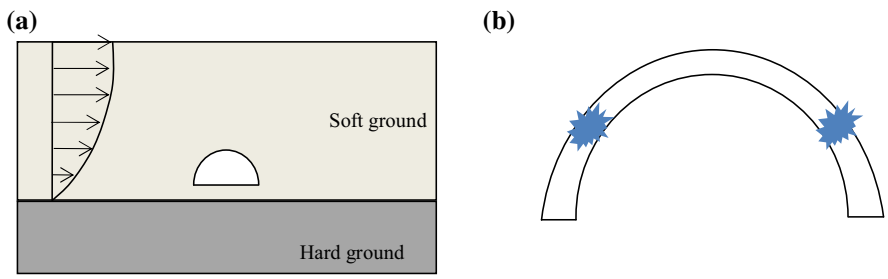

Fig. 12 Vulnerability near junction of hard and soft ground. **a** Amplified ground movement in softer strata, **b** development of crack at junction of shoulder and sidewall

shown in Fig. 12. Such a mechanism is believed to have caused major damages to mountain tunnels as reported by Miyabayashi et al. (2008).

The influence of geological conditions has also been recognized for deeper tunnel sections. Damages observed for the Rokko tunnel during 1995 Hyogoken-Nanbu earthquake at sections having comparatively larger overburden depth are also attributed to the prevailing geological conditions. One of the major findings of the investigation was the fact that almost all the damaged sections were located in highly fractured zone.

6 Plausible Mechanisms of Seismic Damages from Literature

A wide range of tunnel lining failures has been identified based on the case studies of damaged mountain tunnels. A few mechanisms proposed to explain some of them are presented in this section. Figure 13 presents the case of seismic shear wave propagating along the diagonal directions which causes shear stresses on the tunnel cross section as shown by dashed lines. These shear stresses can be resolved into a set of horizontal and vertical stresses subjecting the tunnel cross section to compressive and tensile action. As a result of such an action, compressive failure at the arch crown and shear failure at the arch shoulder may occur.

Figure 14 shows a case in which the diagonal stresses give rise to tensile and compressive forces in the horizontal and vertical direction respectively. Such an action causes the vertical compression of the tunnel cross section coupled with an extension of the sidewalls. Spalling of concrete at the sidewalls may be observed in such a scenario resulting in exposure of lining reinforcements.

With these basic understanding of mechanism of damages, different failure patterns of tunnel lining may be summarized considering seismic wave propagation as discussed below.

6.1 Longitudinal Cracks at Arch Shoulder

The cracking of tunnel lining along the arch shoulder in the longitudinal direction results from vertical

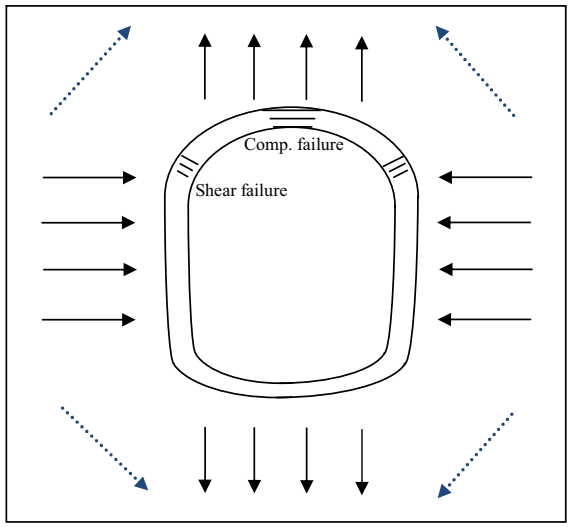

Fig. 13 Mechanism of compressive and shear failure of tunnel lining

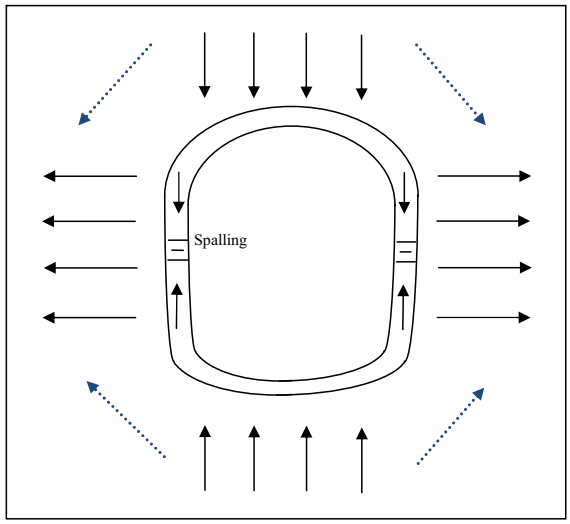

Fig. 14 Mechanism of spalling of tunnel lining

propagation of S-waves parallel to the tunnel cross-section. It causes particle movement in a horizontal direction as shown in Fig. 15 resulting in stress concentration at the junction of the sidewall and the arch.

6.2 Transverse/Circumferential Cracks

Transverse cracks are a result of propagation of P-waves along the direction of tunnel axis. Under this condition, alternate tension and compression along with the pounding of construction joints leads to the development of cracks along the circumference of the tunnel as shown in Fig. 16.

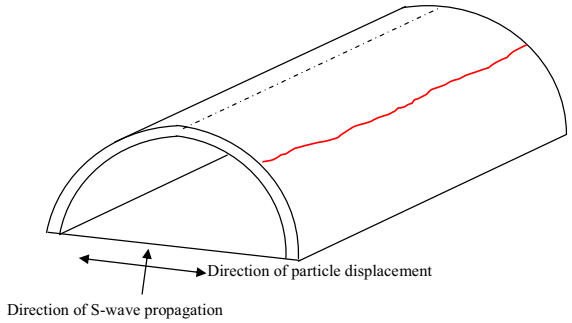

Fig. 15 Longitudinal cracks of tunnel lining

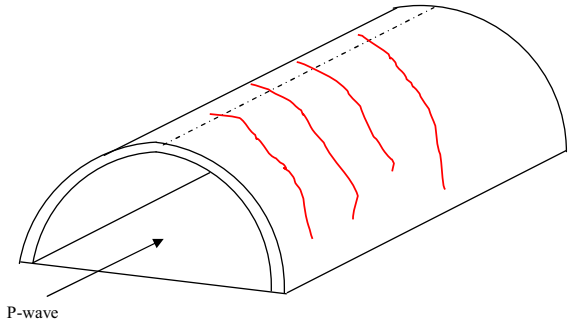

Fig. 16 Transverse crack due to propagation of P-wave along longitudinal direction

6.3 Inclined Cracks

Propagation of S-waves in the vertical direction in a plane parallel to the longitudinal axis of the tunnel results in development of tensile forces resulting in inclined cracks as shown in Fig. 17.

6.4 Pavement Cracks

The pavement cracks are a result of vertical propagation of high frequency P waves parallel to the cross section. Under such wave propagation pattern arching or bending of the bottom pavement occurs as shown in Fig. 18.

6.5 Shear Failure of Lining due to Fault Movement

The shearing failure of tunnel lining results from a relative movement of adjacent parts of the tunnel intersecting the fault plane. Generally the damages

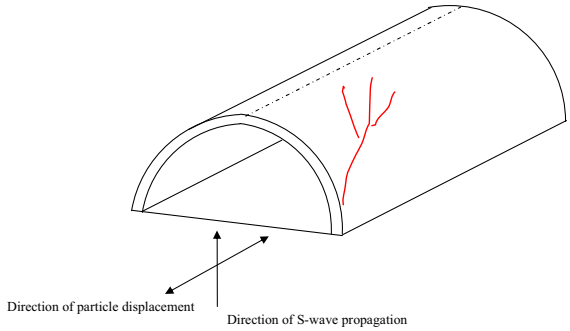

Fig. 17 Inclined cracks due to propagation of S-wave

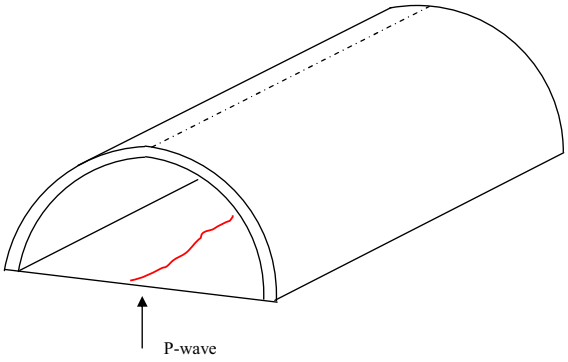

Fig. 18 Cracking of bottom pavement under action of P-wave

sustained in such cases are very severe and may result in complete collapse of the tunnel. Figure 19 illustrates the shear failure of lining induced due to fault movement.

7 Seismic Analysis of Lined Tunnel in Fractured Rock Mass

In the present section, a numerical investigation has been presented dealing with the seismic response of a circular lined tunnel passing through fractured rock mass. The influence of depth of tunnel, frequency and PGA of the dynamic wave on the dynamically induced axial force and bending moment in the tunnel liner has been discussed. The results of the numerical analyses have been corroborated with some of the patterns of seismic damages observed in the past.

7.1 Modeling and Analyses

The numerical modeling of a circular lined tunnel subjected to dynamic loads has been carried out in a discrete element based software package UDEC. The

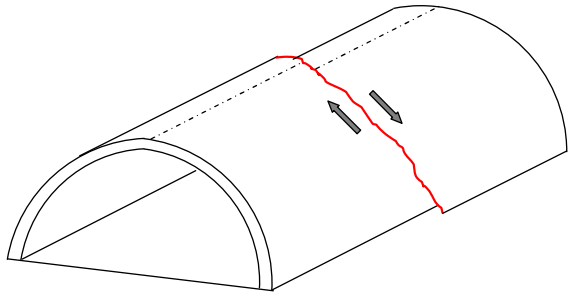

Fig. 19 Shear failure of tunnel lining due to fault movement

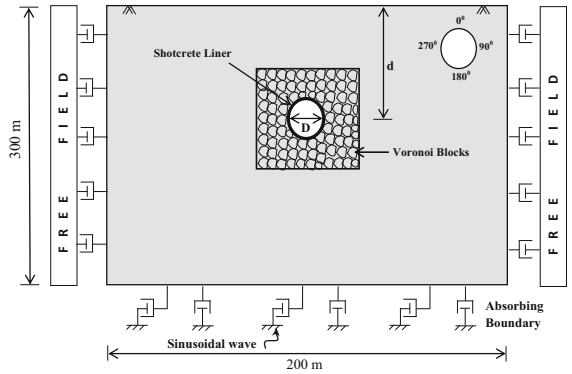

Fig. 20 Schematic representation of numerical model

schematic representation of the numerical model considered in the present study is shown in Fig. 20. The model consists of a circular tunnel having a diameter D (10 m) located at a variable depth of d (75 and 150 m) below the ground surface. To simulate the fractured nature of the rock mass, Voronoi tessellation scheme (Lorig and Cundall 1989) has been used to represent the blocky nature of the rock mass. This feature has been utilized to create randomly sized polygons representing the blocky nature of the medium around the tunnel. Brittle fracturing is allowed to occur along the edge of these Voronoi blocks in the event of either the shear or tensile strength being exceeded. Both the intact rock and the voronoi joints have been modeled using the Mohr–Coulomb constitutive law. The properties adopted in the study have been listed in Table 10. The properties are representative of the fractured nature of rocks encountered in case of real tunnel projects (Lunardi 2008).

The lining around the circular tunnel has been simulated using beam elements. The density of the

Table 10 Properties adopted for numerical model in present study

Property	Intact rock	Rock block interface
Density (kN/m^3)	23	–
Cohesion (MPa)	3	1
Friction angle (°)	35	20
Elastic modulus (GPa)	10	–
Poisson's ratio	0.2	–
Tensile strength (MPa)	0.5	0.0005
Normal stiffness (GPa/m)	–	2.2
Shear stiffness (GPa/m)	–	1.1

liner is 2500 kg/m^3 having an elastic modulus of 30 GPa and Poisson's ratio of 0.2 (Shen et al. 2014) To ensure no slippage between the liner and the surrounding geological medium, the properties of the interface has been set to very high values so as to effectively glue them together (Itasca Consulting Group Inc. 2004). Moreover, elastic behavior has been assumed for the liner.

The mesh size adopted in the numerical model has been finalized based on the following considerations:

1. Efficient simulation of propagation of waveforms of dominant frequency range associated with the adopted sinusoidal motions.
2. Simulation of the stress gradient in the geological medium close to the tunnel structure.

In order to ensure the first condition, the mesh size is kept smaller than 1/10th of the smallest wavelength of interest in the simulation. For meeting the second condition, a finer discretization has been selected for regions close to the tunnel structure which gradually becomes coarser subject to the condition that no distortion of the propagating seismic waves occurs in the simulation.

To minimize adverse boundary effects during dynamic analysis, free field boundary conditions has been invoked at the lateral sides. In addition, viscous dashpots have been used at the bottom boundary in both the normal and shear directions. Moreover, the dimensions of the model have been kept as 200 m (20D) × 300 m (30D) in all the analyses.

The use of dashpots at the bottom boundary requires the dynamic input to be converted into stress waves which has been achieved through Eq. (1).

$$\sigma_s = 2\rho C_s V_s(t) \quad (1)$$

where ρ represents the mass density of the material, *Cs* is the shear wave velocity and *Vs*(*t*) is the instantaneous horizontal input motion velocity. Sinusoidal acceleration with six different frequencies between 1 and 10 Hz has been utilized in the study. Prior to every dynamic analysis, an initial static in situ stress state has been invoked keeping K = 1.0.

7.2 Effect of Depth and Frequency of Input Motion

A plot of typical variation of dynamic axial force and bending moment along the tunnel liner has been shown in Figs. 21 and 22 respectively. It is seen that the variation in the liner axial force and moment is driven by the nature of dynamic input as the recorded response comprises of steady state cycles having sinusoidal nature during the action of the dynamic wave. At the end of the dynamic input, a residual value of force and moment remains in the liner.

The variation of axial forces in the liner for tunnel at depths of 150 and 75 m are shown in Figs. 23 and 24 respectively. It is seen that the forces are greater in case of tunnel at a depth of 150 m. Moreover, the frequency of input motion also has an effect on the maximum axial forces recorded during dynamic analyses (Fig. 23).

For both tunnel depths, the maximum axial force is largest for the case of 1 Hz frequency. A subsequent increase in frequency of input motion shows a decrease in the axial forces. Such a phenomenon maybe attributed to the frequency filtering effect of the

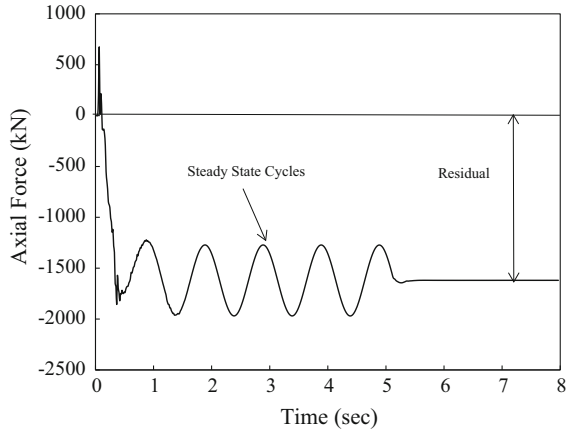

Fig. 21 Typical axial force time history

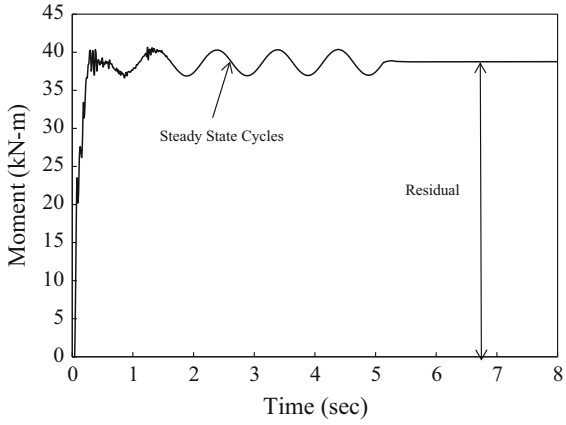

Fig. 22 Typical bending moment time history

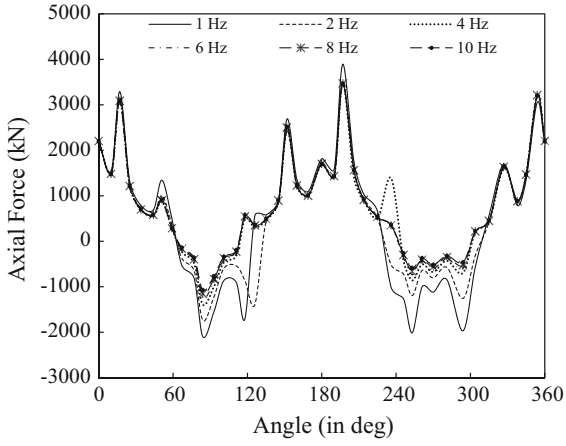

Fig. 23 Maximum dynamic axial force along liner (d = 150 m)

Voronoi joints incorporated in the present numerical model for representation of blocky nature of rock mass. The fractured nature of the rock mass acts as a low pass filter which allows only low frequency waves to pass through and blocks the higher frequency motions (Myer and Pyrak-Nolte 1990; Cai and Zhao 2000; Jiao et al. 2005).

The pattern of joints which have failed either in tension or shear in the vicinity of the tunnel has been shown in Figs. 25 and 26 respectively. Figure 25 corresponds to the case of tunnel at a depth of 150 m subjected to an input frequency of 1 Hz. It is observed that the stress exceeds the strength of the Voronoi joints resulting in development of fractures near the left shoulder and the lower right portion of the tunnel. This phenomenon explains the subsequent higher axial

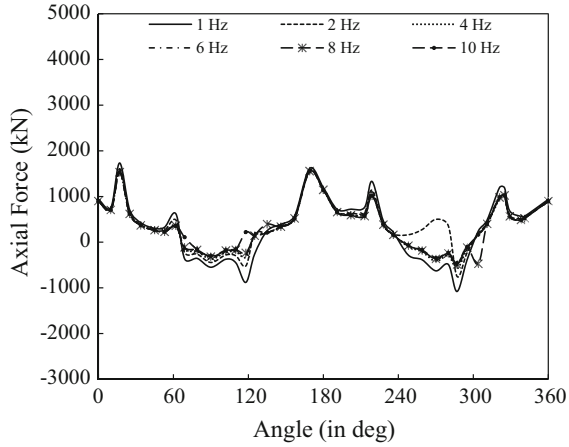

Fig. 24 Maximum dynamic axial force along liner (d = 75 m)

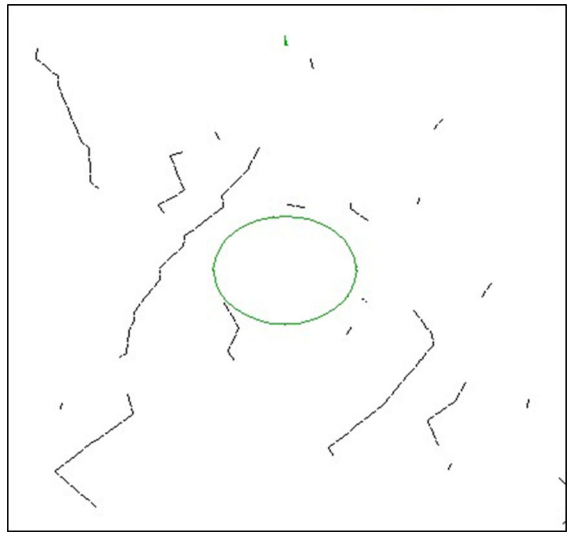

Fig. 25 Failed joint pattern around tunnel (d = 150 m, 1 Hz)

forces recorded in the tunnel liner (Fig. 23) at angles of 70°–120° and 240°–300°. Thus it is inferred with reasonable certainty that the Voronoi blocks replicate the additional degree of freedom associated in case of blocky rock masses resulting in subsequent higher forces (Fig. 27).

In contrast, the stresses along the Voronoi joints do not exceed the strength for the case of tunnel at a depth of 150 m subjected to motion of frequency 6 Hz. This behavior is observed in the failed joint pattern shown in Fig. 26. Similarly, the failure development was minimal for all the cases of tunnel at depth of 75 m suggesting the importance of overburden and the static

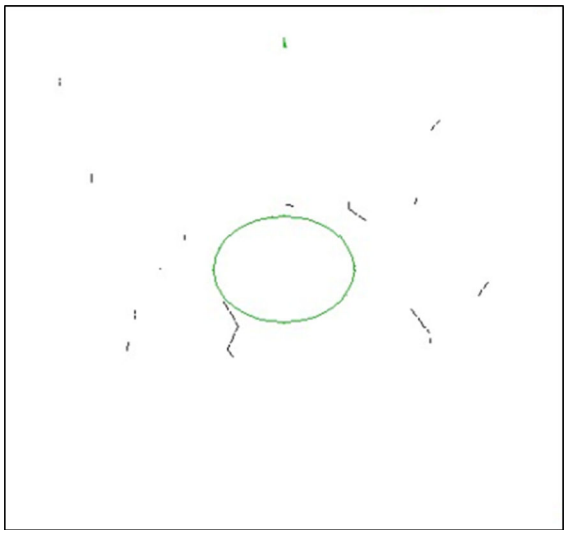

Fig. 26 Failed joint pattern around tunnel (d = 150 m, 6 Hz)

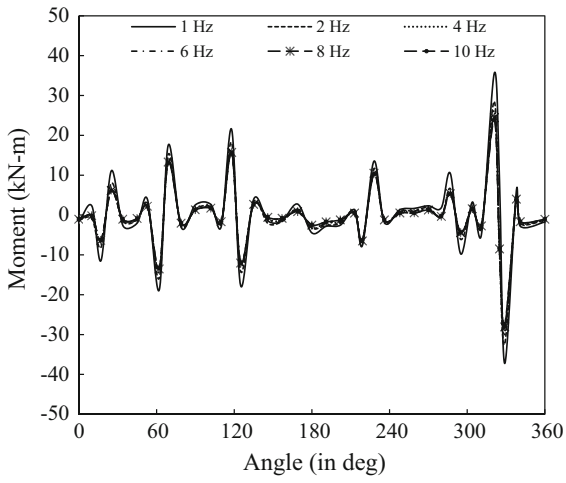

Fig. 27 Maximum dynamic bending moment along liner (d = 75 m)

stresses in governing rock block movements under dynamic action.

Figures 27 and 28 show the variation in maximum bending moment along the liner at various frequencies of input motion for tunnel at depth of 150 and 75 m respectively. It is observed that the moment is also maximum at 1 Hz frequency. However, at higher frequencies, variation of moment is minimal for the various frequencies of input motion considered in the present study.

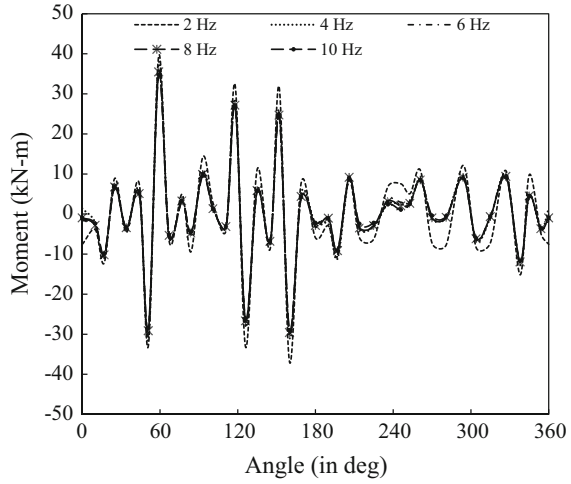

Fig. 28 Maximum dynamic bending moment along liner (d = 150 m)

From the ensuing discussion, it may be noted that deeper tunnel section passing through blocky rock mass subjected to low frequency excitations experiences higher dynamic forces and hence are more prone to damages. This may explain the failure of deep tunnel sections passing through fractured regions which manifest in terms of collapse of secondary concrete lining as reported in literature.

7.3 Effect of Peak Horizontal Acceleration (PHA)

To evaluate the influence of the peak ground motion on the seismic response of tunnels, analyses were carried out by employing sinusoidal motions having PHA of 0.2 and 0.5 g for tunnel located at a depth of 150 m.The analyses have been run for frequencies of 1 and 2 Hz only. The variation of the dynamic axial force in the liner for the case of 0.2 and 0.5 g has been presented in Figs. 29 and 30 respectively. Similarly, Figs. 31 and 32 highlight the variation of bending moment in the liner for excitations having PHA of 0.2 and 0.5 g respectively.

For the case of 1 Hz frequency, it is observed that the maximum dynamic axial force increases by 25 % as the PHA increases from 0.1 to 0.2 g. The percentage increase becomes 54 % when a PGA of 0.5 g is adopted. A similar trend of increase in the dynamic bending moment is noted where an increase of 92 and 271 % is observed for PHA of 0.2 and 0.5 g

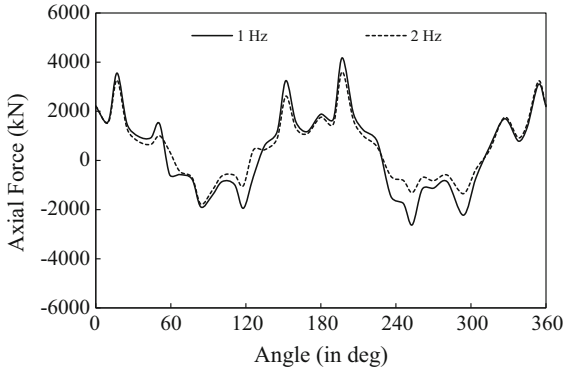

Fig. 29 Maximum dynamic axial force along liner subjected to PHA of 0.2 g

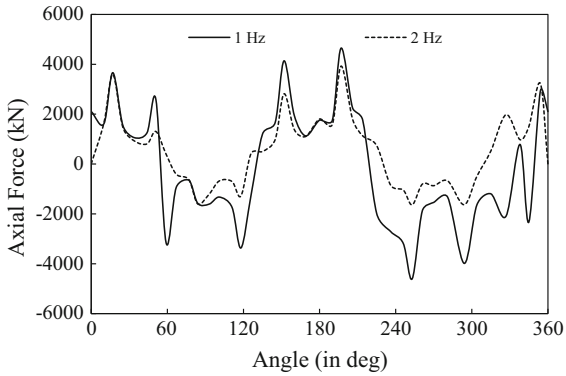

Fig. 30 Maximum dynamic axial force along liner subjected to PHA of 0.5 g

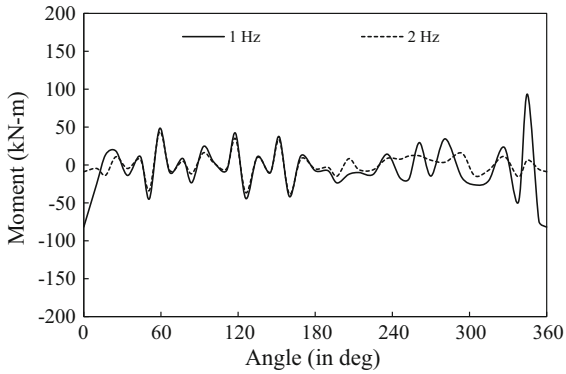

Fig. 31 Maximum dynamic bending moment along liner subjected to PHA of 0.2 g

respectively. Similar trend of increase in the liner forces are observed for the case of 2 Hz. However, the percentage increase is lower in comparison to the case of 1 Hz frequency. Thus, it may be stated that the

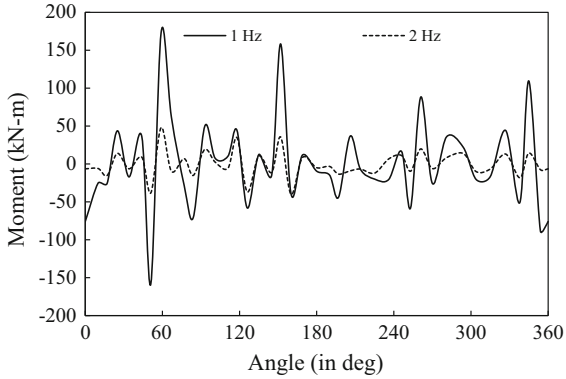

Fig. 32 Maximum dynamic bending moment along liner subjected to PHA of 0.5 g

vulnerability of the tunnels subjected to dynamic loads are higher in case of low frequency motions having higher PHA values. Table 11 summarizes the maximum forces and percentage change for the cases considered in the study.

7.4 Effect of Peak Horizontal Acceleration on Observed Tunnel Damages

Based on the discussions presented in the preceding sections, it can be concluded that one of the major factors affecting damages is the energy reaching the location of the tunnel. In order to predict the level of ground shaking, a number of attenuation laws have been proposed in literature (Kramer 1996). In the present section, the attenuation relation suggested by Campbell (1981) has been used to evaluate the Peak Horizontal Acceleration (PHA) at tunnel locations reported to have been damaged following the 1999 Chi-Chi earthquake and 2008 Wenchuan earthquake. Equation (2) represents the attenuation relation expressing the PHA as a function of epicentral distance (R) and magnitude (M).

$$\ln PGA(g) = -4.141 + 0.868M - 1.09\ln[R + 0.0606\exp(0.7M)] \quad (2)$$

Using Eq. (2), the PHA at tunnel location for the 57 tunnels listed in Table 5 has been evaluated. The results have been summarized in Table 12 relating the number of tunnel damages with the PHA. It is noted that only 3 tunnels suffered damages in case the PHA predicted from the attenuation relation is within 0.1 g. However, a substantial increase of tunnel damages is noted for higher PHA. In a similar manner, the

Table 11 Variation in maximum axial force and bending moment with PHA

Frequency (Hz)	PGA (g)	Axial (+) (in kN)	%	Axial (−) (in kN)	%	Moment (+) (in kN-m)	%	Moment (−) (in kN-m)	%
1	0.1	3894		2098		41		43	
	0.2	4175	7	2623	25	93	56	82	92
	0.5	4650	25	4605	54	173	77	158	271
2	0.1	3509		1739		39		37	
	0.2	3606	3	1780	2	44	10	39	4
	0.5	3925	12	1638	−6	48	21	40	7

Table 12 Damage to tunnels for various PHA in 1999 Chi-Chi earthquake

PHA (g)	Number of tunnels damaged	Percent
Up to 0.1	3	5
0.11–0.2	21	37
0.21–0.3	20	35
0.31–0.4	5	9
0.41–0.5	6	11
0.51–0.6	0	–
0.61–0.7	1	2

Table 13 Damage to tunnels for various PHA in 2008 Wenchuan earthquakes

PHA (g)	Number of tunnels damaged	Percent
Up to 0.1	–	–
0.11–0.2	4	13
0.21–0.3	7	23
0.31–0.4	2	7
0.41–0.5	7	23
0.51–0.6	5	17
0.61–0.7	3	10
0.71–8	2	7

attenuation relation has been applied for the tunnels listed in Table 6 and the results have been summarized in Table 13. It is noted that no case of tunnel damages is observed in case of PHA being within 0.1 g. However, higher PHA of 0.2 g and above is associated with greater number of tunnel damages.

Table 14 combines the results of both the earthquake events of 1999 Chi-Chi and 2008 Wenchuan earthquakes. From Table 14, it can be observed that a PHA of 0.1 g has caused damages to 3 tunnels only. In comparison, a substantial increase in cases of tunnel damages is observed for a PHA of 0.2 g and higher.

Table 14 Summary of damages to tunnels in 1999 Chi-Chi and 2008 Wenchuan earthquake relating PHA

PHA (g)	Number of tunnels damaged	Percent
Up to 0.1	3	3.4
0.11–0.2	25	28.7
0.21–0.3	27	31
0.31–0.4	7	8
0.41–0.5	13	14.9
0.51–0.6	5	5.7
0.61–0.7	4	4.6
0.71–8	3	3.4

These observations compare well with the findings highlighted in Sect. 7.3 where a substantial increase in tunnel liner forces has been observed as the PGA increases from 0.1 to 0.2 g.

8 Summary and Discussion

In the present paper, wide collection of literature reporting seismic damages of mountain tunnels has been reviewed. Some major cases of damages have been highlighted based on which various patterns of instabilities have been recognized. Observations made from damages have clearly shown that tunnels are vulnerable in portal sections, near zones of high impedance contrast or when passing through blocky rock masses. Moreover, important parameters believed to have a major impact on the seismic performance of tunnels have been discussed. A short summary of the probable failure mechanisms proposed in literature has also been presented.

To gain greater insight into the seismic response of tunnels, a numerical investigation of dynamic behavior of circular lined tunnel in blocky rock mass has

been carried out. The roles of frequency of input seismic wave and tunnel depth on the dynamically induced axial force and bending moment in the tunnel liner have been discussed. It is observed that lower frequency waves induce higher axial force in the tunnel liner and lead to greater extent of surrounding rock mass to fail either in tension or in shear. Such behavior may be attributed to the frequency filtering effect which allows only lower frequency waves to pass across them.

In addition, the role of PHA on tunnel vulnerability has also been studied. It is observed that increase in the PHA leads to a consequent increase in the dynamically induced axial force and bending moment in the tunnel liner which may lead to various types of tunnel liner failures. In this context, the PHA at locations of tunnels damaged following two recent earthquakes are evaluated using an attenuation relation. The results compare well with the observations made from the numerical simulations carried out in the present study.

From the review of past seismic damages of mountain tunnels and numerical investigations carried out in this study following major conclusions may be drawn.

- Contrary to the popular belief, mountain tunnels are vulnerable to seismic damages as observed from various damages in tunnels in past earthquakes.
- Frequency content of the earthquake motion is a guiding factor in inducing damage in the tunnel liner. With regard to this, impact of degree of weathering on the properties of blocky rock mass will be crucial in modifying the frequency content of the seismic motion. From the study, it is confirmed that lower frequency ground motion will be having greater effect on the seismic response of tunnels.
- Peak Horizontal Acceleration (PHA) will be a critical parameter governing tunnel damages. Using attenuation relationship, PHA values were evaluated for the tunnels damaged in 1999 Chi-Chi and 2008 Wenchuan earthquakes. It shows good correlation with PHA and tunnel damage. Numerical investigation also confirmed the same.
- The study shows that the increase in tunnel depth will induce more seismic forces in the tunnel liner in case of mountain tunnels especially in blocky rock mass. More investigation, including both field observation as well as numerical investigation is envisaged for coming out with generalized conclusion for the same.

Acknowledgments The first author acknowledges the financial support provided by MHRD, Govt. of India. The authors also appreciate the support from the Head of Department, Department of Civil Engineering, MNIT Jaipur for providing necessary support and assistance. The authors would also like to acknowledge the support of the Department of Earthquake Engineering, IIT Roorkee, for granting the permission to utilize the computing facility to carry out the present study.

References

Asakura T, Sato Y (1996) Damage to mountain tunnels in hazard area. Soils Foundations, Special Issue, pp 301–310

Asakura T, Sato Y (1998) Mountain tunnels in the 1995 Hyogoken-Nanbu earthquake. Q Rep RTRI 39(1):9–16

Brown IR, Brekke TL, Korbin GE (1981) Behavior of the Bay Area Rapid Transit tunnels through the Hayward fault. US Department of Transportation, Urban Mass Transportation Administration. Report UMTA-CA-06-0120-81-1, Washington, DC

Cai JG, Zhao J (2000) Effects of multiple parallel fractures on apparent attenuation of stress waves in rock masses. Int J Rock Mech Min Sci 37(4):661–682

Campbell KW (1981) Near source attenuation of peak horizontal acceleration. Bull Seismol Soc Am 71:2039–2070

Chen Z, Shi Z, Li T, Yuan Y (2012) Damage characteristics and influence factors of mountain tunnels under strong earthquakes. Nat Hazards 61:387–401. doi:10.1007/s11069-011-9924-3

Dowding CH, Rozen A (1978) Damage to rock tunnel from earthquake shaking. J Geotech Eng Div ASCE 104(GT2):175–191

Duke CM, Leeds DJ (1959) Effects of earthquakes on tunnels. In: RAND Protective Construction Symp

Hashash YMA, Hook JJ, Schmidt B, Yao JIC (2001) Seismic design and analysis of underground structures. Tunn Undergr Space Technol 16:247–293. doi:10.1016/S0886-7798(01)00051-7

Huang RQ, Li WL (2009) Analysis of the geo-hazards triggered by the 12 May 2008 Wenchuan earthquake, China. Bull Eng Geol Environ 68:363–371. doi:10.1007/s10064-009-0207-0

Itasca Consulting Group Inc. (2004) Universal Distinct Element Code User's Manual. Minneapolis

Jiang Y, Wang C, Zhao X (2010) Damage assessment of tunnels caused by the 2004 Mid Niigata Prefecture Earthquake using Hayashi's quantification theory type II. Nat Hazards 53:425–441. doi:10.1007/s11069-009-9441-9

Jiao YY, Fan SC, Zhao J (2005) Numerical investigation of joint effect on shock wave propagation in jointed rock masses. J Test Eval 33(3):197–203

Kawakami H (1984) Evaluation of deformation of tunnel structure due to Izu-oshima-kinkai earthquake of 1978. Earthq Eng Struct Dyn 12:369–383. doi:10.1002/eqe.4290120306

Kitagawa Y, Hiraishi H (2004) Overview of the 1995 Hyogo-ken-Nanbu earthquake and proposals for earthquake mitigation measures. J Jpn Assoc Earthq Eng 4(3) (Special Issue)

Konagai K (2005) Data archives of seismic fault-induced damage. Soil Dyn Earthq Eng 25:559–570. doi:10.1016/j.soildyn.2004.11.009

Konagai K, Hohansson J, Zafeirakos A, Numada M, Sadr AA (2005) Damage to tunnels in the October 23, 2004 Chuetsu earthquake. In: Proceedings of the JSCE Earthquake Engineering Symposium vol 28, p 75. doi:10.11532/proee2005a.28.75

Kontoe S, Zdravkovic L, Potts DM, Menkiti CO (2008) Case study on seismic tunnel response. Can Geotech J 45:1743–1764. doi:10.1139/T08-087

Kramer S (1996) Geotechnical earthquake engineering. Prentice Hall Inc., Upper Saddle River

Kumari SDA, Sitharam TG (2012) Tunnels in weak ground: discrete element simulations. ISRM India J 1(1):17–24

Li T (2012) Damage to mountain tunnels related to the Wenchuan earthquake and some suggestions for Aseismic tunnel construction. Bull Eng Geol Environ 71:297–308. doi:10.1007/s10064-011-0367-6

Lorig LJ, Cundall PA (1989) Modeling of reinforced concrete using the distinct element method. In: Fracture of concrete and rock : SEM-RILEM International Conference, June 17–19, 198, Houston, Texas, USA, pp 276–287

Lunardi P (2008) Design and construction of tunnels: analysis of controlled deformation in rocks and soils (ADECO-RS). Springer, Berlin

Miyabayashi H, Tosaka T, Isogai A, Kojima Y, Yashiro K, Saito J, Asakura T (2008) Basic studies on earthquake damage to shallow mountain tunnels. In: Proceedings of the World Tunnel Congress 2008—Underground Facilities for Better Environment and Safety—India

Murano T, Takewaki N (1984) On earthquake resistance of rock caverns. A report prepared for the NEA Coordinating Group on Geological Disposal OECD/NEA

Myer LR, Pyrak-Nolte LJ, Cook NGW (1990) Effects of single fracture on seismic wave propagation. In: Barton N, Stephansson O (eds) Rock Joints. Balkema, Rotterdam, pp 467–473

O'Rourke TD, Goh SH, Menkiti CO, Mair RJ (2001) Highway tunnel performance during the 1999Duzce earthquake. In: Proceedings of the 15th international conference on soil mechanics and foundation engineering, vol 2. Balkema, Rotterdam, pp 1365–1368

Otsuka H, Mashimo H, Hoshikuma J, Takamiya S, Ikeguti M (1997) Damage to underground structures (1995 Hyogoken Nanbu earthquake). J Res 33:481–509

Owen GN, Scholl RE (1980) Earthquake engineering of large under, ground structures. Rep FHWA/RD-80/195, prepared for FHWA 279p, URS/John A Blume and Ass

Penzien J (2000) Seismically induced racking of tunnel linings. Int J Earthq Eng Struct Dyn 29(5):683–691. doi:10.1002/(SICI)1096-9845(200005)29:5<683::AID-EQE932>3.0.CO;2-1

Power MS, Rosidi D, Kaneshiro JY (1998) Seismic vulnerability of tunnels and underground structures revisited. 1998. In: Proceedings of North American Tunnelling'98. Newport Beach, CA: Balkema, Rotterdam, The Netherlands, pp 243–250

Roy N, Sarkar R (2015) Effect of mechanical properties of discontinuity on the seismic stability of tunnels in jointed rock mass. In: Proceedings of the 50th Indian Geotechnical Conference, Pune

Sharma S, Judd WR (1991) Underground opening damage from earthquakes. Eng Geol 30:263–276

Shen Y, Gao B, Yang X, Shuangjiang T (2014) Seismic damage mechanism and dynamic deformation characteristic analysis of mountain tunnel after Wenchuan earthquake. Eng Geol 180:85–98. doi:10.1016/j.enggeo.2014.07.017

Shimizu M, Suzuki T, Kato S, Kojima Y, Yashiro K, Asakura T (2007a) Historical damages of tunnels in Japan and case studies of damaged railway tunnels in the Mid Niigata Prefecture Earthquakes. Underground Space—the 4th Dimension of Metropolis, p 1937

Shimizu M, Saito T, Suzuki S, Asakura T (2007b) Results of survey regarding damages of railroad tunnels caused by the Mid Niigata Prefecture Earthquake in 2004. Tunn Undergr 38(4):265–273

Tao S, Gao B, Wen Y, Zhou X (2011) Investigation and analysis on the seismic damage of mountain tunnels subjected to Wenchuan earthquake. Appl Mech Mater 99–100:273–281. doi:10.4028/www.scientific.net/AMM.99-100.273

Wang ZZ, Zhang Z (2013) Seismic damage classification and risk assessment of mountain tunnels with a validation for the 2008 Wenchuan earthquake. Soil Dyn Earthq Eng 45:45–55. doi:10.1016/j.soildyn.2012.11.002

Wang WL, Wang TT, Su JJ, Lin CH, Seng CR, Huang TH (2000) The seismic hazards and rehabilitation of tunnels in central Taiwan after Chi-Chi earthquake. Sino Geotech 81:85–96

Wang WL, Wang TT, Su JJ, Lin CH, Seng CR, Huang TH (2001) Assessment of damage in mountain tunnels due to the Taiwan Chi-Chi earthquake. Tunn Undergr Space Technol 16:133–150. doi:10.1016/S0886-7798(01)00047-5

Wang ZZ, Gao B, Jiang YJ, Yuan S (2009) Investigation and assessment on mountain tunnels and geotechnical damage after the Wenchuan earthquake. Sci China Ser E Technol Sci 52(2):546–558. doi:10.1007/s11431-009-0054-z

Xu Q, Fan XM, Huang RQ, Westen CV (2009) Landslide dams triggered by the Wenchuan earthquake, Sichuan Province, south west China. Bull Eng Geol Environ 68:373–386. doi:10.1007/s10064-009-0214-1

Yashiro K, Kojima Y (2007) Historical earthquake damage to tunnel in Japan and case studies of railway tunnels in the 2004 Niigataken-Chuetsu earthquake. Q Rep RTRI 48(3):136–141

Yoshikawa K (1981) Investigation about past earthquake disasters of railway tunnels. Q Rep RTRI (Railway Technical Research Institute) 22(3):103–111

Yoshikawa K, Fukuchi G (1984) Earthquake damage to railway tunnels in Japan. In: Adv. Tunnelling Technol. Subsurf. Use v 4 n 31984, Prot of Underground Struct Against Seism Eff Jt Open Sess ITA/SOCVENOS. Caracas, Venezuela, 6 Jun 1984, pp 75–83

Zhang JX (2013) Earthquake mechanics study with health check for a seismic-damaged tunnel suffered from the Wenchuan earthquake. Appl Mech Mater 387:68–71. doi:10.4028/www.scientific.net/AMM.387.68

Zhao X, Li TB, Tao LJ, Hou S, Li LY, Qiu WG (2013) Failure mechanism of tunnel portal during strong earthquakes. Int Efforts Lifeline Earthq Eng. doi:10.1016/9780784413234.041

Zheng WZ, Bo G, YuanJun J, Song Y (2009) Investigation and assessment on mountain tunnels and geotechnical damage after the Wenchuan earthquake. Sci China Ser E Technol Sci 52(2):546–558. doi:10.1007/s11431-009-0054-z

Zheng S, Jiang S, Wang X (2012) Research on the mechanism of earthquake damage of tunnels. Adv Mater Res 538–541:705–708. doi:10.4028/www.scientific.net/AMR.538-541.705